ANALYSIS OF LOCOMOTIVE MOTOR TORQUE IMPACT AT CHANGEABLE DYNAMIC OPERATION CONDITIONS

***A. Atiyah*[1]**

[1] *Faculty of Mechanical Engineering CTU in Prague, ahmad.atiyah@fs.cvut.cz*

Abstract: In today's locomotives, various undesirable dynamic phenomena affect the torque efficiency transmitted to the wheels. The impact of these dynamics ranges from minor effects to major effects that can involve the locomotive as a whole, as in the case of a slip. In this paper, we analysed the behavior of the torque transmitted to wheels during variable levels of adhesion. The results showed a comparison between the motor torque value at different levels of adhesion and its value under normal operat-ing conditions when the adhesion value is at its best.

Keywords: Wheels; Torque; Adhesion; Slip; Asynchronous Motor; Locomotive; Dynamic

1 Introduction

Modern locomotives play an important role in transportation compared with other means of transport, as they are characterized by strength, flexibility, reliability, high performance, and low-cost operation.

These features come with many challenges related to the external and internal dynamics which has a high impact on the traction system. One of these challenges is what is known as the adhesion phenomena, which represents the friction force between the wheels and the rails, and is influenced by the external ambient conditions of the train and the rail condition (wet or dry, etc.).

Another dynamic phenomenon that affects the safe operation o the train is what is known as slip, which occurs when the wheels circumference velocity exceeds the linear speed of the train itself as a result of applying a traction force to the wheels greater than the friction force of the rail itself.

These undesirable dynamic conditions, has a direct impact on the electrical and mechanical systems of the train, in particular the torque of the motor transmitted to the wheels, as the wheels are linked to locomotive traction motor via the gearbox, and when slip occurs, the value of the torque drops significantly due to the decrease in adhesion.

2 Slip and Adhesion

In rail transport, Adhesion is a phenomenon without which it cannot be realized. There is therefore a great interest in its use to the maximum extent possible to increase the efficiency of rail transport. The geometric-kinematic context of adhesion is shown in Fig. 1.

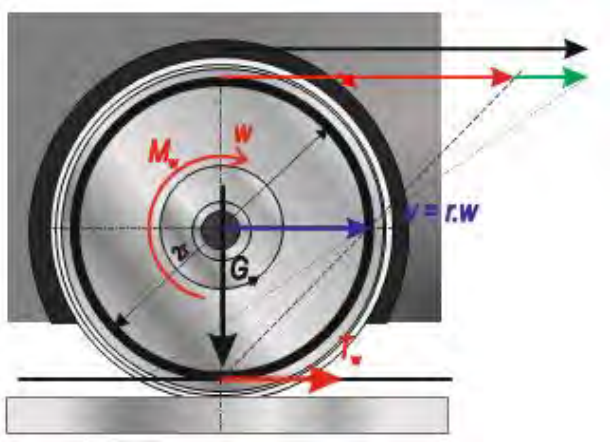

Fig. 1. Context of adhesoin between wheel and rail

In the case of an ideal rolling motion, a wheel of diameter d = 2r rotating at an angular velocity w moves to a distance equal to the circumference of the wheel 2πr in a time equal to T = 2π/w, i.e., that it performs a horizontal motion with speed v = 2πr/(2π/w) = wr.

During train operation, when a decrease in the adhesion between the wheels and the rail occurs, the speed of the wheels increases by slip ratio (r.w-v)/v [2].

The value of the adhesion coefficient depends not only on the wheel slip but it is highly variable according to the conditions prevailing at the point of contact of the wheel with the rail, such as humidity, temperature, pollution by oil, dust, leaves, etc. Its direct on-line evaluation in the normal operation is very difficult.

According to Popovici table shown in Fig.2, In the region of low values of the slip, the adhesion coefficient increases with the increasing value of the slip. Due to the unchanging wheel weight load Gw it means increase of the wheel tangential force, i.e., more effective traction up to certain achievable maximum. It is clear that in an optimal rail vehicle ride should be utilized this maximum, but there must be a protection against an overrun into the area where the increase of the slip leads to a reduction of the adhesion coefficient. A ride under such conditions is unwanted, delivered torque is not used in acceleration wheel turns quicker then it corresponds vehicle movement, adhesions go into friction with all consequences such as wearing and mechanical stress.

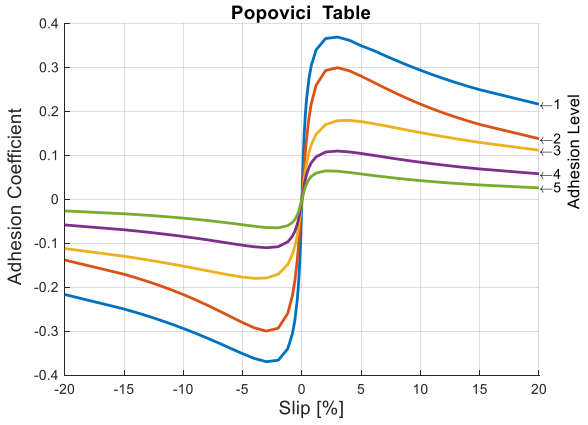

Fig. 2. Adhesion coefficient-Slip characteristics from Popovici table

In order to avoid slip occurrence, usually, locomotives drive unit is equipped with so-called Slip controllers, where it takes the responsibility to regulate (reduce) the asynchronous motor torque in such a way that the slip will be suppressed [1]. In our Simulink model, such a slip controller has been not yet developed, and alternatively, attention was paid to optimize traction motor torque during the loss of adhesion and slip occurrence by analyzing the torque response at changeable adhesion levels and different initial operation conditions, in addition to controlling the motor torque using the vector control method.

3 Asynchronous Motor and Wheelset

The main task of the locomotive wheel-set drive system is ensuring delivering the adequate torque value from the asynchronous motor control system. In case of the absence of sensors that measure the wheel speed, the task of controlling the entire drive system falls to the motor control system, which means that the wheelset velocity is determined by the asynchronous motor velocity which is measured using a sensor mounted at the motor shaft.

It is worth here explaining the mutual relationship between the motor and the wheelset drive system. Thus, when the adhesion value decreases, the speed of the wheels increases by slip ratio. This increase in wheel speed is linked with the asynchronous motor rotational speed through gears. and thus, the motor angular velocity has a direct influence on the internal dynamics and variables behaviors of the asynchronous motor via the so-called motor slip.

The motor angular velocity is used as an input signal to the motor control system. The increase of the wheels speed is matched by a sudden decrease in the value of the torque transmitted to the wheels, and from simulation results, we noticed that the decrease in adhesion value has an impact on both motor rotational velocity and the motor voltage which results in an increase in the voltage value above its nominal value. This also results in an increase in the stator frequency [1].

The significance of this effect becomes apparent if we know that the magnetic flux linkage which has a direct impact on controlling torque must be maintained at a constant value, and this can be achieved by maintaining the motor voltage within the nominal limits. The maximum torque of the asynchronous motor is directly determined by the maximum value of the stator current, as shown in the relation (6). We have observed via simulation experiments, that when the value of adhesion decreases, the decrease in torque is accompanied by a slight decrease in the value of the stator current in order to keep the magnetic flux constant. Since the current is a measured quantity, then, it's good to consider the possibility of early detection of wheel slip by generating a suitable delay for the Anti-slip controller to respond in the case of a continuous decrease in the current value.

In order to achieve the desired dynamics of the locomotive movement, the concern not only includes generating sufficient motor torque but also extends to involve the enhancement of the torque control quality using different control methods. If an inadequate tractive torque is detected, it may lead to an inadequate wheel slip and a subsequent limiting vehicle dynamic.

Studying the different asynchronous motor control methods used in the locomotive drive unit helps in determining the torque behavior of the ASM more effectively, and can also lead to an increase of the locomotive's response to unwanted dynamic changes affect it, and it may even be possible to predict these dynamic changes before they occur.

3.1 Asynchronous Motor Model

The asynchronous motor is considered the main component of a railway locomotive, it is responsible for delivering the adequate torque value to the wheelset in order to let the train move on the rail. In this paper, the ASM model used is controlled only via the FOC method without VSI.

To obtain an ASM model, Clark and park transformation has been used for decades [4][5] to convert the motor equations from three-axis reference coordinates "abc" into a two-axis "αβ0" stationary reference frame or rotating frame “dq0” [6]. There are multiple reasons behind using those transformation methods, one of these reasons is the presence of time-varying inductances in the motor voltage equations [5]. Clark transformation matrix T_c can be expressed by the following equation:

$$T_c = \frac{2}{3}\begin{bmatrix} 1 & -\frac{1}{2} & -\frac{1}{2} \\ 0 & \frac{\sqrt{3}}{2} & -\frac{\sqrt{3}}{2} \end{bmatrix} \qquad (1)$$

and thus, we can easily obtain the $i_{s\alpha}, i_{s\beta}$ currents which are of a sinusoidal nature. To create an efficient control method for ASM, the converted motor quantities using Clark transformation should be of continuous nature, and that can be achieved by means of the Clark to Park transformation matrix represented in the Fig.3 using the following equation:

$$\begin{bmatrix} i_{s,dq} \end{bmatrix} = T_p \cdot \begin{bmatrix} i_{s,\alpha\beta} \end{bmatrix}$$
$$\begin{bmatrix} i_{sd} \\ i_{sq} \end{bmatrix} = \begin{bmatrix} \cos(\gamma_s) & \sin(\gamma_s) \\ -\sin(\gamma_s) & \cos(\gamma_s) \end{bmatrix} \cdot \begin{bmatrix} i_{s\alpha} \\ i_{s\beta} \end{bmatrix} \qquad (2)$$

Where is i_{sd}, i_{sq} are the stator currents in rotating reference frame rated in [A].

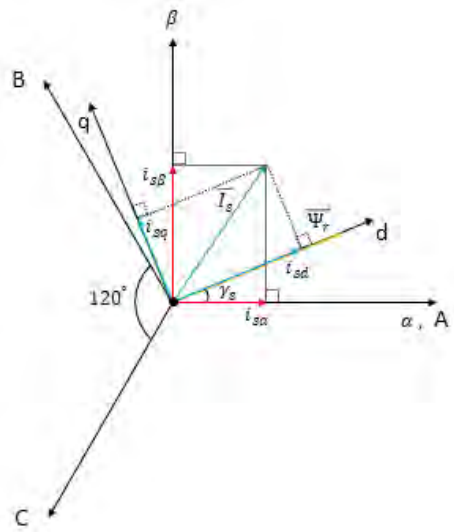

Fig. 3. Stator Current space vector in stationary and rotating reference frames

The stator and rotor voltages in stationary frame can be written as follows:

$$\begin{aligned} u_{s\alpha}(t) &= r_s i_{s\alpha}(t) + \frac{d}{dt}\psi_{s\alpha}(t) \\ u_{s\beta}(t) &= r_s i_{s\beta}(t) + \frac{d}{dt}\psi_{s\beta}(t) \\ 0 = u_{r\alpha}(t) &= r_r i_{r\alpha}(t) + \frac{d}{dt}\psi_{r\alpha}(t) + \omega_m p_p \cdot \psi_{r\beta}(t) \\ 0 = u_{r\beta}(t) &= r_r i_{r\beta}(t) + \frac{d}{dt}\psi_{r\beta}(t) - \omega_m p_p \cdot \psi_{r\alpha}(t) \end{aligned} \tag{3}$$

The equation which gives the electromechanical torque of an asynchronous motor can be expressed as follows:

$$M(t) = \frac{3}{2} p_p \cdot (\psi_{r\alpha}(t) \cdot i_{s\beta}(t) - \psi_{r\beta}(t) \cdot i_{s\alpha}(t)) \tag{4}$$

Where $M(t)$ represent the electromechanical torque rated in [N.m].

3.2 Field Oriented Control

So far, a variety of vector modelling methods like FOC and DTC [3][7][8][9] has been used in practice to control the ASM.

For long time, FOC considered as the most common method to control AC motor in practice. FOC control method is represented using what is known as direct quadratic coordinates (*dq0* coordinates), and this coordinate system rotates synchronously with rotor flux vector. In FOC, the torque is proportional to the cross product of stator current and flux vector. By decoupling the torque and flux vectors form each other, the control of both torque and flux is quite similar to DC motor control. In our Simulink model, we developed an ASM control based on FOC. The torque vector is aligned with q-axis, and the flux vector is aligned with d-axis, which result in:

$$\psi_r = \begin{bmatrix} \psi_{rd} \\ \psi_{rq} \end{bmatrix} = \begin{bmatrix} |\psi_r| \\ 0 \end{bmatrix} \tag{5}$$

And hence $\psi_{rq} = 0$, the motor torque can be rewritten as:

$$M(t) = \frac{3}{2} p_p \cdot \psi_{rd}(t) \cdot i_{sq}(t) = \frac{3}{2} p_p \cdot |\psi_r(t)| \cdot i_{sq}(t) \tag{6}$$

We can notice from equation (6), that we can control the motor torque with stator current i_{sq} by keeping the rotor flux at a constant value [10]. Fig.3 shows the FOC block diagram of ASM.

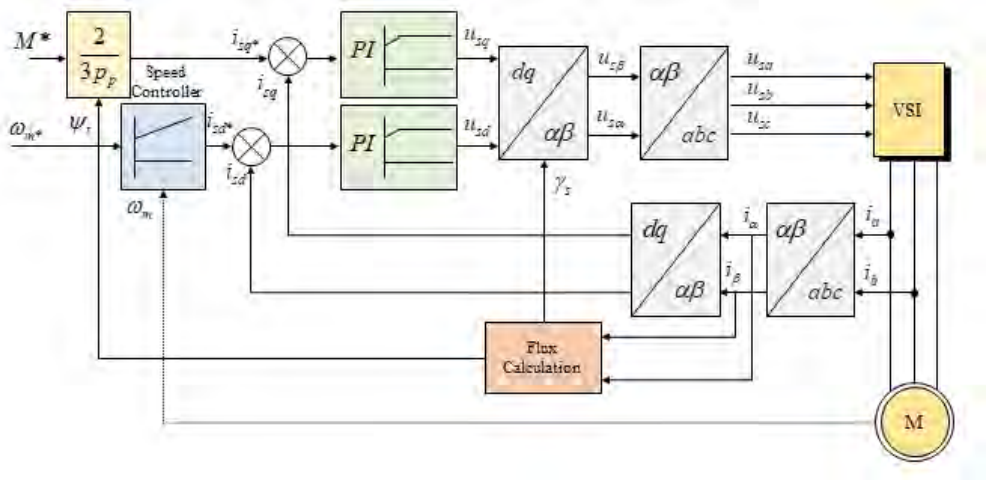

Fig. 4. Block diagram of asynchronous motor

From Fig.4, two PI controllers are used to regulate the *dq* stator currents. The PI output voltages are transformed to stationnary voltages using inverse Park to Clark transformation matrix:

$$\left[u_{s,dq}(t)\right] = T_p \cdot \left[u_{s,\alpha\beta}(t)\right]$$
$$\begin{bmatrix} u_{s\alpha}(t) \\ u_{s\beta}(t) \end{bmatrix} = \begin{bmatrix} \cos(\gamma_s) & -\sin(\gamma_s) \\ \sin(\gamma_s) & \cos(\gamma_s) \end{bmatrix} \cdot \begin{bmatrix} u_{sd}(t) \\ u_{sq}(t) \end{bmatrix} \quad (7)$$

We can convert the resulting stationary U_{sd}, U_{sq} voltages to 3-phase voltages by means of Clark inverse matrix.

4 Simulation Results

So far, our Simulink model has satisfied the mechanical part, while the electrical part is still subject to further development in order to optimize the motor torque and enhance the countability of the locomotive drive.

The asynchronous motor model used is modelled according to the parameters of a real ML4550-K / 6 motor which has a maximum torque of 10000N.m[11]. A numerical simulation has been carried out using Matlab/Simulink to show how motor torque transmitted to the wheels at different operation conditions and under undesired dynamics changes.

Table 1, shows the parameter values for the simulation experiments. the torque value was set to a range of 4200-8400 N.m at a normal operating velocity of 100 km.h^{-1} and at a low operating velocity of 10 km.h^{-1}.

All simulation experiments were performed in two stages, in the first stage, no variable adhesion levels are taken into account. While in the second stage, the values of adhesion levels were changed from 1 - 5, which are shown in Fig.2.

The initial train velocity is of Step signal, while the torque setpoint is a ramp signal.

Tab. 1. Simulation parameters of the traction motor

Simulation Test	Longitudinal Velocity km/h	Torque N.m	Adhesion Level	Adhesoin Time
I	100	4200	1	4.5-9.5-14.5-17.5
II	100	4200	1-5	
III	100	8400	1	
IV	100	8400	1-5	
V	10	4200	1	
VI	10	4200	1-5	
VII	10	8400	1	
VIII	10	8400	1-5	

From Fig.5(a), we notice that when a 4800 Nm torque setpoint is applied at a speed of 100 km.h^{-1} with no change in the adhesion level, the motor torque tracks the desired torque setpoint with a negligible steady-state error, and the response speed of the motor torque relative to the desired torque setpoint is fast with a low torque ripples amplitudes transmitted to the wheels. When changing the adhesion levels according to the simulation times shown in Table 1, we noticed a significant decrease in the motor torque ranges between 56 - 159 Nm as shown in Fig.5(b).

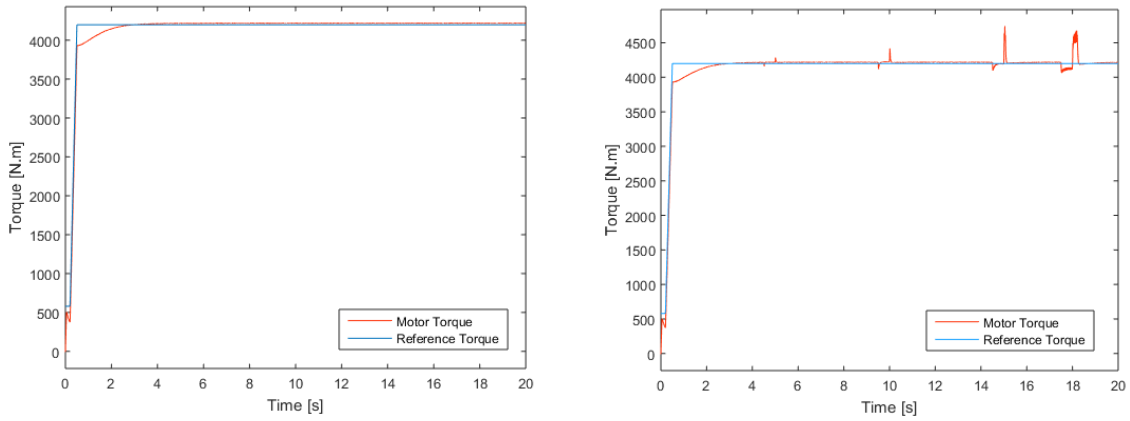

(a). (b).

Fig. 5.a) Motor torque response at 4200N.m and 100km.h^{-1} with no adhesion changes.
b) Motor torque response at 4200N.m and 100km.h^{-1} with changeable adhesion levels

By setting the desired torque value at 8400 N.m which represents the nominal value of the locomotive motor torque at an operating speed of 100 km.h^{-1} and without changing the adhesion level, the motor torque is unable to track the desired torque value. This could be clearly shown in Fig.6(a), where the steady-state error increases gradually with time elapsed. When changing the adhesion level from 1-5, we noticed a significant decrease in the motor torque value at the adhesion levels (2-3), and a severe non-linear drop in its value at the adhesion level 5, which represents a case of slip occurrence in the locomotive wheels at Rail contact as shown in Fig.6(b).

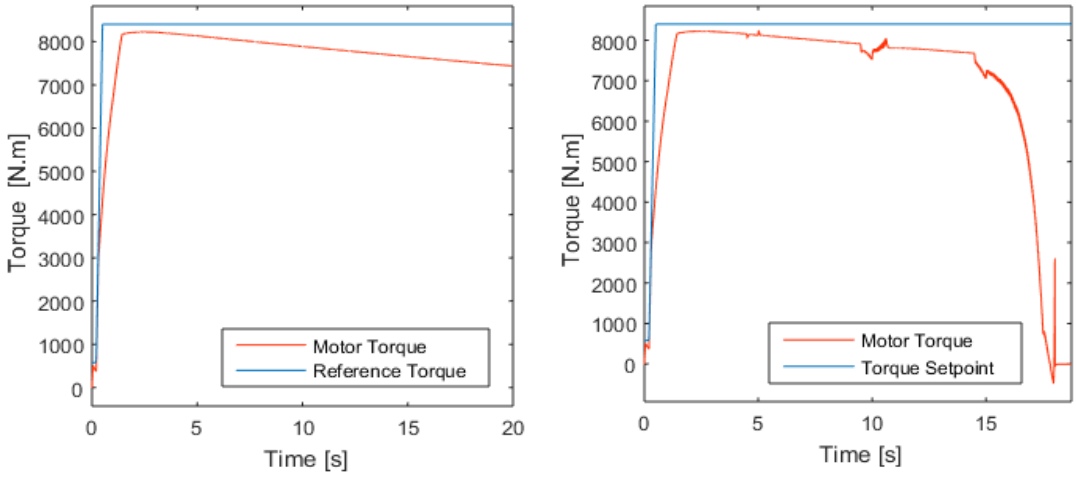

(a). (b).

Fig. 6.a) Motor torque response at 8400N.m and 100km.h^{-1} with no adhesion changes
b) Motor torque response at 8400N.m and 100km.h-1 with changeable adhesion levels

At low operating speeds of the locomotive at 10 km.h^{-1}, with desired torque value of 4200 N.m without changing the adhesion levels, the motor torque response is as shown in Fig.7(a), where the motor torque response speed is slower compared to the torque response in Fig.5(a).

When changing the adhesion levels, we noticed that the motor torque failed to track the desired torque value at the fifth level which represents the worst adhesion value as shown in Fig.7(b).

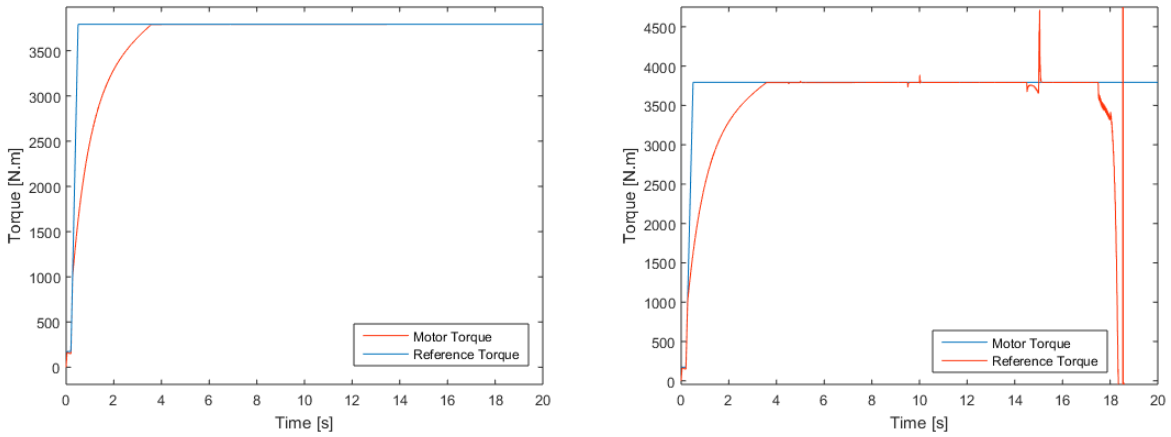

(a). (b).

Fig. 7.a) Motor torque response at 4200N.m and 10km.h^{-1} with no adhesion changes
b) Motor torque response at 4200N.m and 10km.h^{-1} with changeable adhesion levels

When we set a torque value of 8400N.m at a speed of 10 km.h^{-1} without changing the adhesion level, we noticed a very slow response of the motor torque related to the desired torque value as shown in Fig.8(a). By changing the adhesion levels, we noticed a nonlinear decrement in the motor torque when the fourth adhesion level is reached, which reflects an occurrence of slip as shown in Fig.8(b).

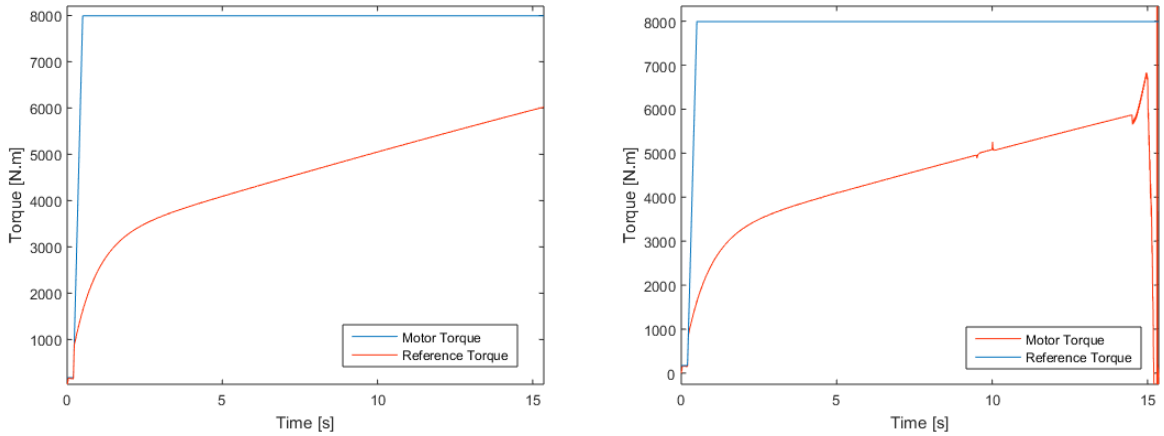

(a). (b).

Fig. 8.a) Motor torque response at 8400N.m and 10km.h^{-1} with no adhesion changes
b) Motor torque response at 8400N.m and 10km.h^{-1} with changeable adhesion levels

5 Conclusion

Studying the effect of the torque dynamic behavior of the asynchronous motor at specific operating conditions on the dynamics of the locomotive such as the movement of its wheels, taking into account changes in the adhesion conditions provides us with the possibility of early detection of dynamic phenomena occurrence such as slip.

Thus, this may help us to develop the current simulation model to include the possibility of optimizing locomotive motor torque and make it able to adapt to changing driving and operating conditions.

The simulation results address the importance of obtaining an appropriate motor control model capable of meeting the changing driving requirements of the traction motor.

acknowledgement

Work has been supported by the SGS grant 19/158/OHK2/3T/12.

Symbols

The symbols used in this paper are listed as follows.

$i_{s,dq}$ stator current in rotary frame (A)
$i_{s,\alpha\beta}$ stator current in stationary frame (A)
$u_{s,dq}$ stator voltage in rotary frame (V)
$u_{s,\alpha\beta}$ stator voltage in stationary frame (V)
$\psi_{s,dq}$ stator flux linkage in rotary frame (Wb)
$\psi_{s,\alpha\beta}$ stator flux linkage stationary frame (Wb)
$i_{r,dq}$ rotor current in rotary frame (A)
$i_{r,\alpha\beta}$ rotor current in stationary frame (A)
$u_{r,dq}$ rotor voltage in rotary frame (V)
$u_{r,\alpha\beta}$ rotor voltage in stationary frame (V)
$\psi_{r,dq}$ rotor flux linkage in rotary frame (Wb)
$\psi_{r,\alpha\beta}$ rotor flux linkage stationary frame (Wb)
r_s stator resistance (Ω)
r_r rotor resistance (Ω)
ω_m angular speed (rad.s^{-1})
$M(t)$ electromechanical torque (N.m)

References

[1] Y. Shimizu, K. Ohishi, T. Sano, S. Yasukawa, and T. Koseki, "*Antislip re-adhesion control based on disturbance observer considering bogie vibration*," in Proc. Eur. Conf. Power Electron. Appl., 2007, pp. 1–10.

[2] P. Pichlik and J. Zdenek, "*Locomotive velocity estimation for a slip control purpose by an unscented Kalman filter*," 2017 18th International Scientific Conference on Electric Power Engineering (EPE), 2017, pp. 1-5, doi: 10.1109/EPE.2017.7967287.

[3] R. Souad and H. Zeroug, "*Comparison between direct torque control and vector control of a permanent magnet synchronous motor drive,*" 2008 13th International Power Electronics and Motion Control Conference, 2008, pp. 1209-1214, doi: 10.1109/EPEPEMC.2008.4635433.

[4] W. C. Duesterhoeft, M. W. Schulz and E. Clarke, "*Determination of Instantaneous Currents and Voltages by Means of Alpha, Beta, and Zero Components,*" in Transactions of the American Institute of Electrical Engineers, vol. 70, no. 2, pp. 1248-1255, July 1951, doi: 10.1109/T-AIEE.1951.5060554.

[5] R. H. Park, "*Two-reaction theory of synchronous machines generalized method of analysis-part I,*" in Transactions of the American Institute of Electrical Engineers, vol. 48, no. 3, pp. 716-727, July 1929.

[6] Paul C. Krause; Oleg Wasynczuk; Scott D. Sudhoff, , "*Analysis of Electric Machinery and Drive Systems*", IEEE, 2002.

[7] Takahashi, I.; Noguchi, T. "*A New Quick-Response and High-E_ciency Control Strategy of an Induction Motor*". IEEE Trans. Ind. Appl. 1986, IA-22, 820–827.

[8] Depenbrock, M. "*Direct self-control (DSC) of inverter fed induktion machine*". In Proceedings of the 1987 IEEEPower Electronics Specialists Conference, Blacksburg, VA, USA, 21–26 June 1987; pp. 632–641.

[9] Casadei, D.; Serra, G.; Stefani, A.; Tani, A.; Zarri, L. "*DTC drives for wide speed range applications using a robust flux-weakening algorithm*". IEEE Trans. Ind. Electron. 2007, 54, 2451–2461.

[10] R. Garg, P. Mahajan, N. Gupta and H. Saroa, "*A comparative study between field oriented control and direct torque control of AC traction motor,*" International Conference on Recent Advances and Innovations in Engineering (ICRAIE-2014), Jaipur, 2014, pp. 1-6.

[11] https://www.skoda.cz/produkty/lokomotivy/rychlikove-lokomotivy/

Selected article from
Tento dokument byl publikován ve sborníku

Nové metody a postupy v oblasti přístrojové techniky, automatického řízení a informatiky 2021

New Methods and Practices in the Instrumentation, Automatic Control and Informatics 2021

15. 9. – 17. 9. 2021, Žatec

ISBN 978-80-01-06889-2

Web page of the original document:
http://iat.fs.cvut.cz/nmp/2021.pdf

Obsah čísla/individual articles:
http://iat.fs.cvut.cz/nmp/2021/

Ústav přístrojové a řídicí techniky, FS ČVUT v Praze, Technická 4, Praha 6